Vector multi-soliton operation and interaction in a graphene mode-locked fiber laser

Yu Feng Song,[1] Lei Li,[1] Han Zhang,[2] De Yuan Shen,[3] Ding Yuan Tang,[1,3,*] and Kian Ping Loh[2]

[1]*School of Electrical and Electronic Engineering, Nanyang Technological University, 639798 Singapore*
[2]*Department of Chemistry, National University of Singapore, 117543 Singapore*
[3]*School of Physics and Electronic Engineering, Jiangsu Normal University, 221116 China*
[*]*edytang@ntu.edu.sg*

Abstract: We experimentally investigated the vector multi-soliton operation and vector soliton interaction in an erbium doped fiber laser passively mode locked by atomic layer graphene. It is found that the vector multi-soliton operation exhibited several characteristic modes. These are the random static distribution of vector solitons, stable bunches of vector solitons, restless oscillations of vector solitons, rain of vector solitons, and emission of a so-called "giant vector soliton". The formation mechanisms of the operation modes were also experimentally investigated.

OCIS codes: (060.4370) Nonlinear optics, fibers; (060.5530) Pulse propagation and temporal solitons.

References and links

1. D. Y. Tang, L. M. Zhao, B. Zhao, and A. Q. Liu, "Mechanism of multisoliton formation and soliton energy quantization in passively mode-locked fiber lasers," Phys. Rev. A **72**(4), 043816 (2005).
2. P. Grelu and J. M. Soto-Crespo, "Temporal soliton molecules in mode-locked lasers: collisions, pulsations and vibrations," in *Dissipative solitons: from optics to biology and medicine*, N. Akhmediev and A. Ankiewicz, eds. (Springer-Verlag, 2008).
3. P. Grelu and J. M. Soto-Crespo, "Multisoliton states and pulse fragmentation in a passively mode-locked fibre laser," J. Opt. Soc. Am. B. **6**(5), S271–S278 (2004).
4. N. Akhmediev and A. Ankiewicz, eds., *Dissipative Solitons: From optics to biology and medicine* (Springer, Berlin-Heidelberg, 2008), Lecture Notes in Physics, V 751.
5. M. Olivier, V. Roy, M. Piché, and F. Babin, "Pulse collisions in the stretched-pulse fiber laser," Opt. Lett. **29**(13), 1461–1463 (2004).
6. M. Grapinet and Ph. Grelu, "Vibrating soliton pairs in a mode-locked laser cavity," Opt. Lett. **31**(14), 2115–2117 (2006).
7. L. M. Zhao, D. Y. Tang, H. Zhang, and X. Wu, "Bunch of restless vector solitons in a fiber laser with SESAM," Opt. Express **17**(10), 8103–8108 (2009).
8. D. Y. Tang, W. S. Man, H. Y. Tam, and P. D. Drummond, "Observation of bound states of solitons in a passively mode-locked laser," Phys. Rev. A **64**(3), 033814 (2001).
9. S. Chouli and P. Grelu, "Soliton rains in a fiber laser: An experimental study," Phys. Rev. A **81**(6), 063829 (2010).
10. S. Chouli and P. Grelu, "Rains of solitons in a fiber laser," Opt. Express **17**(14), 11776–11781 (2009).
11. J. W. Haus, G. Shaulov, E. A. Kuzin, and J. Sanchez-Mondragon, "Vector soliton fiber lasers," Opt. Lett. **24**(6), 376–378 (1999).
12. S. T. Cundiff, B. C. Collings, and W. H. Knox, "Polarization locking in an isotropic, modelocked soliton Er/Yb fiber laser," Opt. Express **1**(1), 12–21 (1997).
13. V. V. Afanasjev, "Soliton polarization rotation in fiber lasers," Opt. Lett. **20**(3), 270–272 (1995).
14. M. N. Islam, C. D. Poole, and J. P. Gordon, "Soliton trapping in birefringent optical fibers," Opt. Lett. **14**(18), 1011–1013 (1989).
15. R. Gumenyuk and O. G. Okhotnikov, "Temporal control of vector soliton bunching by slow/fast saturable absorption," J. Opt. Soc. Am. B **29**(1), 1–7 (2012).
16. Q. Bao, H. Zhang, Y. Wang, Z. Ni, Y. Yan, Z. X. Shen, K. P. Loh, and D. Y. Tang, "Atomic-layer graphene as a saturable absorber for ultrafast pulsed lasers," Adv. Funct. Mater. **19**(19), 3077–3083 (2009).
17. D. Popa, Z. Sun, F. Torrisi, T. Hasan, F. Wang, and A. C. Ferrari, "Sub 200 fs pulse generation from a graphene mode locked fiber laser," Appl. Phys. Lett. **97**(20), 203106 (2010).

#185787 - $15.00 USD Received 25 Feb 2013; revised 29 Mar 2013; accepted 31 Mar 2013; published 15 Apr 2013

18. L. M. Zhao, D. Y. Tang, H. Zhang, X. Wu, Q. Bao, and K. P. Loh, "Dissipative soliton operation of an ytterbium-doped fiber laser mode locked with atomic multilayer graphene," Opt. Lett. **35**(21), 3622–3624 (2010).
19. A. Reina, X. Jia, J. Ho, D. Nezich, H. Son, V. Bulovic, M. S. Dresselhaus, and J. Kong, "Large area, few-layer graphene films on arbitrary substrates by chemical vapor deposition," Nano Lett. **9**(1), 30–35 (2009).
20. S. M. J. Kelly, "Characteristic sideband instability of periodically amplified average soliton," Electron. Lett. **28**(8), 806–807 (1992).
21. H. Zhang, D. Y. Tang, L. M. Zhao, and N. Xiang, "Coherent energy exchange between components of a vector soliton in fiber lasers," Opt. Express **16**(17), 12618–12623 (2008).
22. D. Y. Tang, B. Zhao, L. M. Zhao, and H. Y. Tam, "Soliton interaction in a fiber ring laser," Phys. Rev. E Stat. Nonlin. Soft Matter Phys. **72**(1), 016616 (2005).
23. Y. F. Song, H. Zhang, D. Y. Tang, and Y. Shen, "Polarization rotation vector solitons in a graphene mode-locked fiber laser," Opt. Express **20**(24), 27283–27289 (2012).

1. Introduction

Multiple soliton formation in mode locked fiber lasers is a well-known phenomenon and has been extensively investigated in the past [1–3]. It has been shown that various mechanisms could lead to the formation of multiple solitons. These include the wave-breaking effect, the effective spectral filtering effect, the soliton peak clamping effect, and the soliton shaping of dispersive waves. Due to the existence of gain and losses in a laser, strictly speaking, all the solitons formed in a fiber laser are essentially the dissipative solitons [4], whose dynamics is governed by the extended complex Ginzburg-Landau equation (CGLE). However, depending on the laser operation conditions, e.g. in a soliton peak clamped case where the formed solitons have a spectral bandwidth which is far narrower than the effective gain bandwidth, the effect of the laser gain is supposed to purely balance the cavity losses, it was experimentally found that the features of the formed solitons are more close to those of the nonlinear Schrödinger equation (NLSE) type of solitons. Theoretically, the NLSE type of solitons is conservative in nature, while those of the CGLE type of solitons are dissipative in nature. They have very different features in soliton interaction. In a passively mode locked fiber laser, through finely controlling the laser operation conditions, one can actually fine tune the properties of the formed solitons, consequently, experimentally control the mutual soliton interaction.

Indeed, in previous experimental studies on the multiple solitons formed in the fiber lasers, people have observed various modes of multiple soliton operation, such as soliton bunches, soliton collisions [5], vibration of soliton pairs [6], restless solitons [7], bound state of solitons [8] and so on. Some of these effects can be traced back as a result of the direct soliton interaction of the dissipative solitons, or the dispersive waves mediated NLSE type of soliton interaction. Therefore, based on the different features of the multiple soliton operation of a fiber laser, one can get an insight into the properties of the formed solitons. Recently, a novel form of multiple soliton operation named as "soliton rain" was observed by Grelu et al. [9, 10]. It was shown that the multiple soliton formation in a fiber laser could even manifest the process of the rain-drop formation in the nature, or in another word, the multiple soliton interaction in a fiber laser follows the universal statistics of the many body systems.

However, most of the previous experimental studies on the multiple soliton operation of fiber lasers were focused on fiber lasers passively mode-locked with the nonlinear polarization rotation (NPR) technique. As to achieve the self-started mode locking of fiber lasers with the NPR technique, a polarizer or an equivalent component is inserted in the laser cavity, which fixes the polarization of the formed solitons everywhere in the cavity, the solitons formed in the fiber lasers thus have no polarization dynamics. Hence, from the dynamics point of view, they are equivalent to that of the scalar solitons. Multiple vector solitons, which are solitons with two orthogonally coupled polarization components, can also be formed in a mode locked fiber laser if polarization sensitive components are removed from the cavity [11]. The formation of vector solitons in a fiber laser is the result of the vector nature of light propagation in the single mode fibers. Therefore, compared with the scalar

#185787 - $15.00 USD Received 25 Feb 2013; revised 29 Mar 2013; accepted 31 Mar 2013; published 15 Apr 2013

solitons, they have more complicated dynamics, e.g. depending on the laser operation conditions people have experimentally observed the polarization locked vector solitons, polarization rotation vector solitons, and the group velocity locked vector solitons [12–14].

The main challenge for achieving vector multi-soliton operation of a fiber laser is to find an appropriate saturable absorber that has polarization insensitive saturable absorption. Initially, the semiconductor saturable absorber mirror (SESAM) was used for the study of multiple vector soliton operation of fiber lasers [7, 15]. In an experiment with a SESAM as the passive mode locker Zhao et al. have observed a state of so-called bunched restless vector solitons [7]. Vector soliton bunching controlled by SESAMs with different recovery times was also experimentally investigated by R. Gumenyuk et al. [15]. Recently, the mode locking of fiber lasers with atomic-layer graphene based saturable absorbers has attracted considerable attention of research [16–18]. The atomic layer graphene based saturable absorbers can have polarization independent saturable absorption [16]. In addition, compared with the SESAMs, they have further a number of novel characteristics, e.g. their saturable absorption has super broad bandwidth and ultrafast recovery time, which render that the formed multiple vector solitons could have many new dynamic features.

In this paper we report on the experimental studies of the multiple vector soliton operation of an erbium doped fiber laser mode-locked with the atomic-layer graphene. We show experimentally that depending on the laser cavity design and the concrete laser operation conditions, different characteristic modes of the multiple soliton operation could be obtained in the vector soliton fiber lasers. Similar modes of the multiple soliton operation have also been observed previously on the scalar soliton fiber lasers [1]. Worth mentioning is that in our experiment vector soliton rains with either the polarization locked or the polarization rotating vector solitons were revealed, which clearly shows the complication of the vector solitons compared with the scalar solitons. Under strong pumping a state of “giant pulse” emission was always obtained in our laser. Such a state of multiple soliton operation was frequently observed in passively mode locked soliton fiber lasers but its formation mechanism and properties were not well studied.

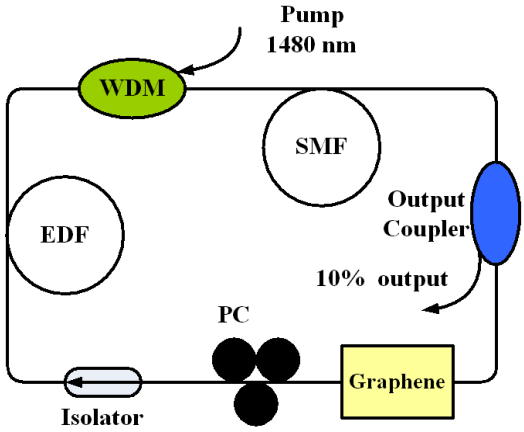

Fig. 1. A schematic diagram of the fiber ring laser. SMF: Single-mode fiber, PC: Polarization controller, EDF: Erbium doped fiber, WDM: Wavelength-division multiplexer.

2. Experimental setup

The schematic of the graphene mode-locked fiber ring laser is shown in Fig. 1. The fiber laser had a ring cavity with a length of 22.6 m. Among the cavity fibers a piece of 0.7 m highly erbium doped fiber (Liekki Er80-8/125) with anomalous dispersion was used as the gain medium. Other fibers used were the standard single mode fiber (SMF28) with a GVD parameter of 18 (ps/nm)/km. A polarization independent isolator was employed in the cavity

#185787 - $15.00 USD Received 25 Feb 2013; revised 29 Mar 2013; accepted 31 Mar 2013; published 15 Apr 2013

to force the unidirectional operation of the ring cavity, and an intra-cavity polarization controller (PC) was used to fine-tune the linear cavity birefringence. The laser was pumped by a high power fiber Raman Laser source (KPS-BT2-RFL-1480-60-FA) of wavelength 1480 nm. The pump laser can deliver a maximum pump power as high as 5 W. A 10% output coupler was used to output the laser emission. The atomic layer graphene used was synthesized with the chemical vapor deposition method [19]. The graphene sheets were carefully deposited on the end facet of an optical fiber, which was inserted in a FC/APC connector. An optical spectrum analyzer (ANDO AQ6317) was used to observe the optical spectra in the frequency domain. A 33 GHz high-speed oscilloscope (Agilent DSA-X 93204A) together with two 45 GHz photo-detectors (New focus 1014) was used to measure the pulse trains in the time domain.

3. Experimental results and discussions

3.1 Bunches of multiple vector solitons

Mode locking of the laser was obtained whenever the pump power was increased to ~80 mW. Multiple solitons were always formed initially in the cavity. A typical state of the multiple solitons immediately after the mode locking is shown in Fig. 2(a). The solitons were randomly distributed in the cavity but they were not static. The solitons moved slowly in the cavity and eventually came together, forming a soliton bunch in the cavity, as shown in Fig. 2(b). After the soliton bunch was formed, the laser then operated in a stable state, and the same soliton bunch repeated with the cavity repetition rate on the oscilloscope trace. Figure 2(c) shows a zoom-in structure of the stable soliton bunch. In the particular case there were 11 solitons in the bunch. The separation between the solitons was not constant and the average distance was ~1 ns. Figure 2(d) shows the corresponding optical spectra of the laser emission. The central wavelength of the solitons was at 1563.6 nm, and the 3 dB bandwidth was ~2.3 nm. Two sets of spectral sidebands appeared on the spectra. The one indicated by arrows was the Kelly sidebands. It confirmed that the mode locked pulses were solitons [20]. Apart from the Kelly sidebands, there was another set of sidebands. The set of sidebands exhibits peak-dip alteration in the polarization resolved spectra, whose appearance was a result of the coherent energy exchange between the two polarization components of the vector solitons [21]. Therefore, based on the characteristic optical spectra (particularly the additional peak-dip spectral sidebands) one can easily determine if the vector solitons are formed. It is noted that these extra sidebands always appeared on the spectra of the mode locked pulses, suggesting that the as-formed solitons were always vector solitons. Except the spectral sidebands, the optical spectra profile was smooth. The state of vector soliton bunch was very stable. It could last several hours if no laser operation conditions were changed. Figure 2(e) shows the measured autocorrelation trace of the solitons. The measured pulse width was 1.8 ps. If a sech^2 pulse profile is assumed, the actual pulse width was about 1.17 ps. The time bandwidth product of the pulses is 0.335, indicating that the pulses are transform-limited. A state of single vector soliton in cavity was obtained through carefully reducing the pump power to ~30 mW. The energy of a single vector soliton of the laser is estimated to be ~8 pJ.

#185787 - $15.00 USD Received 25 Feb 2013; revised 29 Mar 2013; accepted 31 Mar 2013; published 15 Apr 2013

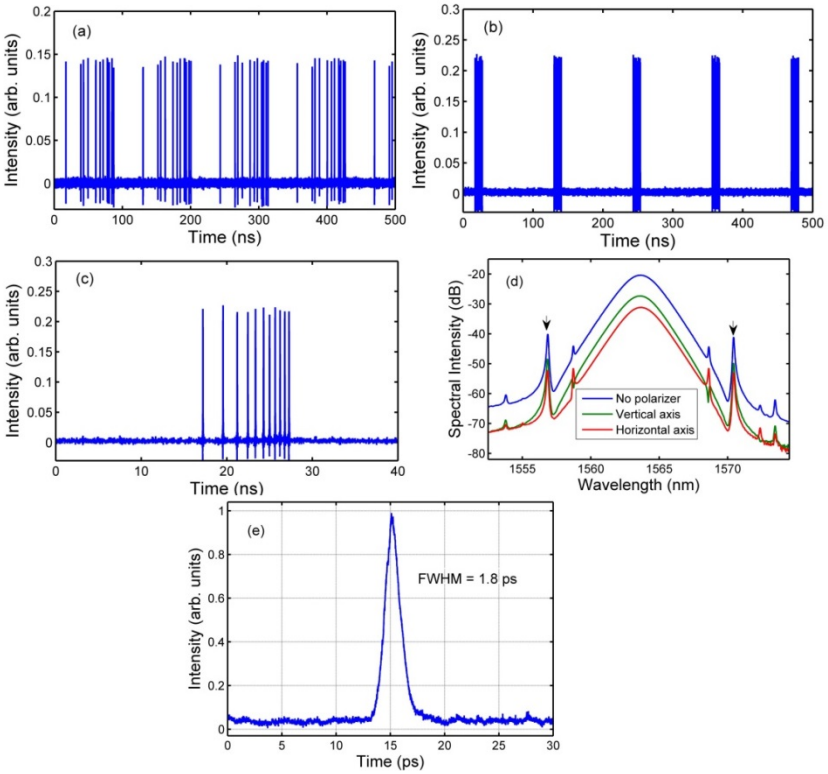

Fig. 2. A typical multiple vector soliton bunch state of the fiber laser. (a) and (b) the oscilloscope trace; (c) the details of the soliton bunch; (d) Polarization resolved optical spectra. Blue line: the total output; Red line: along the horizontal axis; Green line: along the vertical axis. (e) Autocorrelation trace.

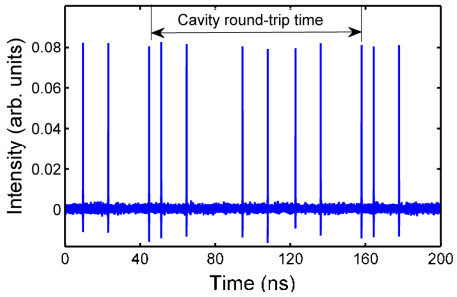

Fig. 3. Random static vector soliton distribution at a low pump power.

3.2 Random static distribution of vector soliton

By tuning the paddles of the PC but without introducing any unstable CW components, a vector soliton bunch could explode. Subsequently a state of steady random vector soliton distribution over the whole cavity was obtained. Figure 3 shows a typical example. There were 7 solitons coexisting in the cavity and they are far apart from each other. The state shown was obtained under a pump power of ~50 mW. If the pump power was then increased, a CW spectral component appeared on the soliton spectrum, indicating that a CW background would be introduced into the cavity. In this case the solitons started to move in the cavity due to the CW mediated soliton-soliton long distance interaction force. Once the CW component was suppressed through carefully reducing the pumping, another state of randomly distributed multiple vector soliton could be obtained. Similar phenomena were also observed previously

#185787 - $15.00 USD Received 25 Feb 2013; revised 29 Mar 2013; accepted 31 Mar 2013; published 15 Apr 2013

on the multiple scalar soliton fiber lasers [22]. It shows that the unstable CW beam provides a global soliton interaction mechanism among the vector solitons formed in a laser.

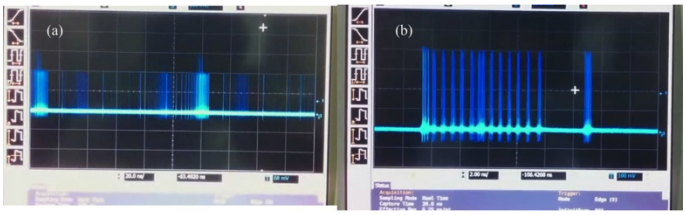

Fig. 4. Bunch of restless vector solitons (video). (a) Soliton bunch moving in the cavity (Media 1); (b) Solitons oscillating in the bunch (Media 2).

3.3 Restless vector soliton

At a relatively stronger pump power (~130 mW), as a result of unstable CW component in the cavity an initially stable state of randomly distributed multiple solitons was destroyed and the solitons started to move in the cavity and eventually formed a soliton bunch. However, the vector solitons in the bunch were not static, but moved constantly with respect to each other, forming a so-called restless vector soliton bunch. A similar restless vector soliton bunch was also observed in a SESAM mode locked fiber laser by Zhao et al. [7]. As the saturable absorption properties of SESAM differ from those of the graphene only in that they have different recovery time and saturable absorption strength, it is not surprising why similar multiple vector soliton operation could be obtained in the graphene mode locked fiber lasers. In our experiments two different types of the restless vector soliton evolutions were observed. Figure 4 (Media 1 and Media 2) shows these two types of the restless vector soliton evolutions, respectively. Figure 4(a) shows the movement of one vector soliton bunch. The soliton bunch moved as a unit in the cavity, while some solitons within in the bunch moved at different velocities. Therefore, vector soliton collisions occurred as indicated by the appearance of the high intensity peaks in the pulse train. Despite of the collisions among the vector solitons, the solitons could not escape from the bunch. The collision among the solitons became more frequent with the increase of the pump power. Figure 4(b) shows a record of another restless vector soliton bunch, where no soliton collisions occurred. However, the relative soliton positions within the bunch varied.

3.4 Vector soliton rain

If the pump power was further increased, the number of solitons formed in the cavity continuously increased. At an appropriate PC setting, an interesting dynamic pattern as shown in Fig. 5(a) could be obtained. In the scalar soliton lasers such a state was called “soliton rain” [9]. The state was called as “soliton rain” because when measured with a low speed detection system, the soliton pulse train in one cavity length could be phenomenally considered as composed of two parts: a soliton flow part (the left hand side of the screen) and a soliton condensed part (the right hand side of the screen), and the solitons are constantly moving from the soliton flow part to the soliton condensed part, which is analogous to the process of rain droplet formation (evaporation from the noisy background/falling to the condensed part) in the nature. As can be seen in Fig. 5(b), when measured with our high-speed detection system the soliton condensed phase is actually a bunch of solitons close to each other. It was experimentally observed that stronger pump power could induce higher density of the solitons within the bunch. Figure 5(c) shows a soliton rain state obtained at the pump power of 200 mW. Not only more solitons were formed in the train but also a large pulse was formed at the end of the flow. The large pulse was a result of the soliton collision within the train. It is worth noting that all the solitons in the train are constantly moving. Figure 5(d) (Media 3) shows a record of the state.

#185787 - $15.00 USD Received 25 Feb 2013; revised 29 Mar 2013; accepted 31 Mar 2013; published 15 Apr 2013

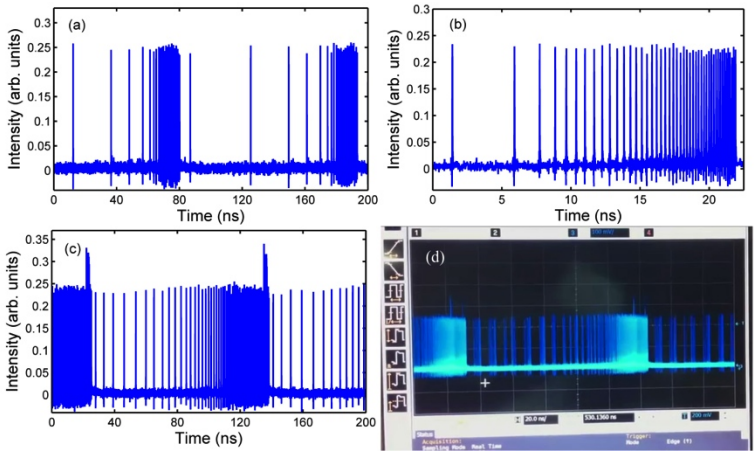

Fig. 5. Polarization locked vector soliton rains: (a) A typical soliton rain at a pump power of 140 mW; (b) zoom-in of the soliton condense phase; (c) Soltion rain at a pump power of 200 mW; (d) Video record of the vector soliton rain (Media 3).

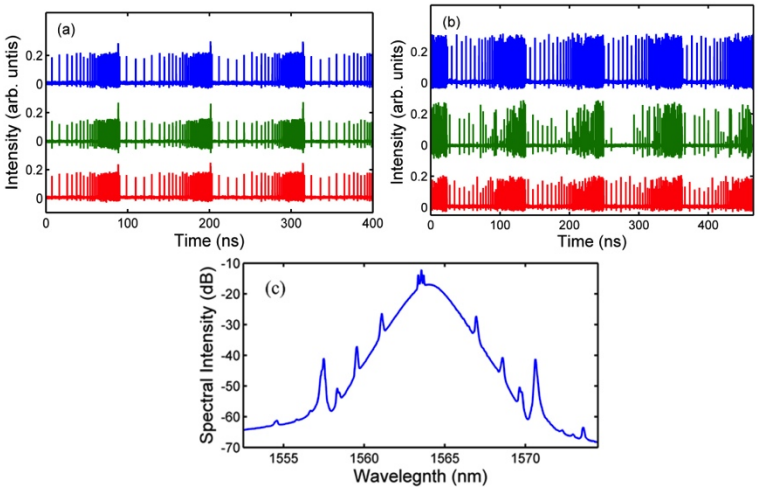

Fig. 6. (a) Oscilloscope traces of the polarization locked vector soliton rain. Blue line: the total output; Green line: along the horizontal axis; Red line: along the vertical axis. (b) Oscilloscope traces of the polarization rotating vector soliton rain. Blue line: the total output; Green line: along the horizontal axis; Red line: along the vertical axis. (c) The optical spectrum of the polarization rotating vector soliton rain.

The main difference between the vector solitons and scalar solitons is that a vector soliton has two coupled orthogonal polarization components. Depending on their coupling the polarization of the vector solitons could be either fixed or rotating [12, 13]. Therefore, different from the scalar soliton rain, by using the polarization resolved measurement technique we are able to identify two different types of vector soliton rains, the polarization locked and polarization rotation vector soliton rains. Figure 6(a) shows the case of the polarization locked vector soliton rain. It can be clearly seen that all the solitons in the flow are uniform both in the total output and the polarization resolved outputs, which is a feature of the polarization locked vector solitons. Figure 6(b) was obtained by slightly changing the setting of the polarization controllers from that of a polarization locked vector soliton rain state. In this way a polarization rotation vector soliton rain state could be obtained. Comparing with Fig. 6(a), it can be seen while all the solitons have the same pulse heights in the total output, the soliton pulse height varied periodically in the polarization resolved

#185787 - $15.00 USD Received 25 Feb 2013; revised 29 Mar 2013; accepted 31 Mar 2013; published 15 Apr 2013

outputs, indicating that the solitons are polarization rotating vector solitons. In particular, the polarization of the vector solitons restore the original polarization every triple of the cavity round-trip time. Polarization rotation of the vector soltions could also be identified from their soliton spectra. Figure 6(c) shows the corresponding optical spectrum of the solitons shown in Fig. 6(b). On the spectrum two extra sets of spectral sidebands could be observed, which were caused by the polarization rotation of the vector solitons in the laser cavity, as shown previously [23].

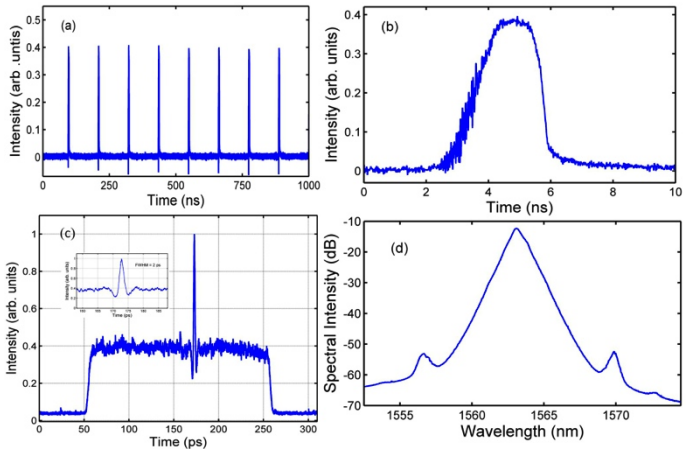

Fig. 7. A giant pulse state obtained at 200 mW pump power. (a) Oscilloscope trace; (b) High-speed measurement of the giant pulse; (c) Autocorrelation trace (inset: zoom-in of the trace); (d) Optical spectrum.

3.5 "Giant pulse" state

When the pump power is high enough (~200 mW), under an appropriate PC setting another multiple vector soliton operation state as shown in Fig. 7 could be observed. Figure 7(a) shows a typical oscilloscope trace of the state. It displayed as a stable pulse train, and each pulse could have very large pulse energy. In our experiment pulse energy as large as 60 nJ had been obtained. Figure 7(b) shows the single pulse profile measured with our high-speed detection system. As the pump power increased the pulse width also increased, but the pulse peak power only increased slightly. Figure 7(c) shows the autocorrelation trace of the pulses. It has an obvious pedestal. On top of the pedestal there is a pulse peak with pulse duration of about 1.29 ps, which is similar to that measured in the multiple vector soliton state. Figure 7(d) shows the optical spectrum of the pulses. It has a triangular shape with blurred spectral sidebands. Based on the measured autocorrelation trace and the pulse spectrum, we conclude that that pulses consist of many tightly packed solitons with random soliton separations.

3.6 Discussions

It is to note that similar multiple soliton patterns have also been observed in the scalar soliton fiber lasers, which shows that the formation of these multiple soliton patterns is a general feature of the soliton lasers, which is independent on whether they are scalar or vector solitons. In a previous paper on the scalar soliton interaction in the passively mode locked fiber lasers we have shown that the various modes of the multiple scalar soliton operation could be traced back to the specific features of the soliton interaction in the cavity [22]. Experimentally, we found that the same is valid for the vector solitons. Despite of the fact that a vector soliton consists of two orthogonally coupled polarization components, and therefore has more complicated dynamics than that of a scalar soliton, the interaction between the vector solitons in a fiber laser cavity is still mainly determined by the same types of interactions mechanisms: the unstable CW caused global type of soliton interaction, the

#185787 - $15.00 USD Received 25 Feb 2013; revised 29 Mar 2013; accepted 31 Mar 2013; published 15 Apr 2013

dispersive wave mediated long range soliton interaction, and the direct soliton interaction, in the fiber lasers that are mode locked by the saturable absorbers like the SESAM or graphene, there is also a absorber caused attraction force, whose strength and action range depends on the saturable absorption strength and the recovery time of the saturable absorbers. The various modes of the vector soliton operation are actually the combined consequence of the mutual actions of these soliton interaction mechanisms on the solitons formed in the laser cavity, e.g. under the effects of a weak unstable CW in the cavity and the saturable absorber effect, the multiple solitons would always have the tendency of soliton bunching. Depending on the strength of the dispersive waves generated by the solitons, one would expect that the solitons in a bunch could be either static or moving restlessly. A soliton rain state could be considered as a special case of the soliton bunch formed under strong pumping, where a lot of solitons are formed in the cavity. A state of bound solitons is formed due to the direct soliton interaction [22]. So far in our experiments no stable states of the closely bound vector soltions have been observed. Nevertheless, we believe that the "giant pulse" state could be formed as a result of the direct soliton interaction in the laser. However, in the current case many solitons are bound together with random soliton separations, therefore, leading to the observed features of the multiple vector soliton laser emission.

4. Conclusions

In conclusion, we have experimentally studied the multiple vector soliton operation of a graphene mode locked fiber laser, and observed various characteristic operation modes of the multiple vector soliton operation of the laser, these include the vector soliton bunches, random static vector soliton distribution, restless vector soliton bunches, "giant pulse" emission, and vector soliton rains. Different from the case of scalar soliton rain, either the polarization-locked vector soliton rain or the polarization rotation vector soliton rain was further identified. Based on results of the experimental studies, we point out that the appearance of the different modes of the multiple vector soliton operation could be well understood by the soliton interaction caused by the following four types of main mechanisms, the unstable CW related global type of soliton interaction, the dispersive wave mediated long range soliton interaction, the direct soliton interaction, and the saturable absorber induced soliton-soliton attraction. Our experimental results demonstrate that in terms of the soliton interaction in the laser cavity both the vector solitons and the scalar solitons show similar features.

Acknowledgments

This project is supported by the funds of Priority Academic Program Development of Jiangsu Higher Education Institutions (PAPD), China and Minister of Education (grant no. 35/12), Singapore.

#185787 - $15.00 USD Received 25 Feb 2013; revised 29 Mar 2013; accepted 31 Mar 2013; published 15 Apr 2013